

## 13A.2

### PRELIMINARY RESULTS FROM THE FIELDING OF A DISPARATE TRIAD OF MOBILE DOPPLER RADARS TO STUDY SEVERE CONVECTIVE STORMS

Howard B. Bluestein\*, Robin Tanamachi, Michael French, Jana Houser, and Jeff Snyder  
University of Oklahoma, Norman, Oklahoma

Robert Bluth and Jeff Knorr  
Naval Postgraduate School, Monterey, California

Ivan Popstefanija, Bethany Seeger, and Chad Baldi\*\*  
ProSensing, Inc., Amherst, Massachusetts

Stephen Frasier and Pei-Sang Tsai  
University of Massachusetts, Amherst, Massachusetts

## 1. INTRODUCTION

Owing to the strong impact they have and to their relatively small size, severe convective storms and tornadoes have been worthy objects of studies using mobile Doppler radars. Since one size does not fit all, a number of different radars have been used, each having a different objective. A W-band radar has been used to probe tornado structure because it requires a relatively small antenna to achieve very high spatial resolution (e.g. Bluestein et al. 2007a). X-band radars have been used to provide storm-scale views of convective storms and, when close enough and when large enough, details of tornado structure, with much less limitation from attenuation than radars at W-band. A polarimetric, X-band radar has been used to distinguish between rain and debris in tornadoes (Bluestein et al. 2007b). It can also be used to distinguish among hydrometeor types.

Based on studies of tornadogenesis (references omitted here for brevity), using mobile radars at both X-band and W-band, it has been shown how not only is high spatial resolution necessary, but so is relatively high temporal resolution. Tornadogenesis precedes on time scales of  $\ll \sim 1$  min, on time scales of 10 s or even less. Mechanically scanning mobile radars usually take 1 min or more to scan a volume covering much of the parent storm. Other techniques, such as electronic scanning, can afford more-rapid scanning.

The purpose of this paper is to describe the results from a field experiment held in May and very early June 2007 in the Plains of the U. S., in which two mobile, X-band Doppler radars were used (a third radar, the UMass W-band radar, was not available in time for field operations; the “triad” part of the title of this paper is no longer valid!).

## 2. RADARS USED

The following two radars were used: An X-band,

\* *Corresponding author address:* Howard B. Bluestein, School of Meteorology, Univ. of Oklahoma, Norman, OK 73072; e-mail: [hblue@ou.edu](mailto:hblue@ou.edu)

\*\* *Former affiliation:* Univ. of Mass., Amherst



Figure 1. MWR-05XP in the Texas Panhandle on 21 May 2007 scanning an approaching squall line. View is to the northwest. Photograph © H. Bluestein.



Figure 2. UMass X-Pol scanning a supercell in the Oklahoma Panhandle on 31 May 2007. View is to the N from a location WNW of Guymon, OK, S of Elkhart, KS, at 1928 CDT. Photograph © H. Bluestein.

phased-array, Doppler radar from the Center for Interdisciplinary Remotely-Piloted Aircraft Studies (CIRPAS) at the Naval Postgraduate School in Monterey, CA (Fig. 1), and a polarimetric, X-band, Doppler radar from the Microwave Remote Sensing Laboratory (MISRL) at the Univ. of Mass. (UMass) at Amherst (Fig. 2).

### 2.1 MWR-05XP

The unique aspect of this field experiment was the use, for the first time, of a mobile phased-array radar, the MWR-05XP (Mobile Weather Radar, 2005, X-band, Phased-Array). The radar is a modified military tactical radar, reconfigured for mobile operation from a heavy-duty truck. In 2007, the radar was mechanically scanned in azimuth over a full 360° and electronically scanned in elevation. This radar can scan a volume covering 360° in azimuth at eight elevation angles in ~ 16 s. Frequency agility, a unique capability of the MWR-05XP, provides an increased number (10 – 32) of independent samples within the same image integration time, thus significantly improving its sensitivity. Other (unclassified) specifications are found in Table 1. More detailed information can be found in Sandifer (2005) and elsewhere. The signals can be oversampled in azimuth, elevation angle, and range. In 2007 it took ~ 10 min to deploy the radar and 8 min to un-deploy.

Transmitted frequency	9.37 – 9.99 GHz
Maximum power	23 kW
Beamwidth	1.8° (azimuth), 2° (elevation)
Max. unambiguous velocity	± 78.1 m s <sup>-1</sup>
Max. PRF	10 kHz
Range resolution	150 m

Table 1. Some characteristics (not actual best system capabilities) of MWR-05XP.

### 2.2 UMass X-Pol

The other radar, known as UMass X-Pol, has been used before (cited earlier), but has been upgraded to include a real-time display for both reflectivity and Doppler velocity, and to operate via battery power. This system is built around a commercial marine radar (using a magnetron); students have gained valuable experience working on both the hardware and software of the radar system. The polarimetric variables differential reflectivity ( $Z_{DR}$ ), cross correlation coefficient ( $\rho_{HV}$ ), and differential phase ( $K_{DP}$ ) are processed later.

The specifications of this radar and additional details are given elsewhere (e.g., Bluestein et al. 2007b). In brief, the beamwidth of the antenna is 1.2°, the range resolution is 150 m, and with staggered PRFs of 1.6 and 2.4 kHz, the maximum unambiguous velocity is ± 38.4 m s<sup>-1</sup>. It takes about 1 – 1.5 min to execute a volume scan of a storm up to 15 – 20° in elevation, in 1° increments, beginning at ~ 3° (to get above ground clutter)..

## 3. CASES

In this brief summary, we present sample data from one case involving data collected by MWR-05XP and in the other we present data from another case involving data collected by the UMass X-Pol. The purpose of this presentation is to highlight the capabilities of each radar.

Date	MWR-05XP	UMass X-Pol	Description
4 May		X	Greensburg, KS tornadic supercell: > 1 h data
5 May		X	SW KS; supercells
6 May		X	SW OK; squall line
8 May	X		Cen. OK; rotating storm N of meso- scale vortex in an MCS
11 May	X	X	Norman, OK; unicellular, ordinary conv.
21 May	X	X	TX Panhandle; squall line
22 May	X	X	N Cen. KS; supercell
23 May	X	X	NW OK, supercell; TX Panhandle, HP supercell and line with book- end vortices
24 May	X		S Cen. OK; squall line MCS
31 May	X	X	OK Panhandle; HP supercell
1 June	X	X	NW TX, HP supercell and a squall line
6 June	X		Cen. NE; squall line

Table 2. List of cases, what radars were used for each case and where, and a brief example of what was scanned. (The radars were also used on other days, but mainly for practice or testing.)

All significant cases are listed in Table 2, along with other pertinent information. In the following section, we show data from a high-precipitation (HP) supercell that produced a tornado while both radars were moving from one deployment site to another (31 May) and data from a supercell that produced a number of tornadoes, one of which devastated Greensburg, KS (4 May). The former case is important because it demonstrates that the MWR-05XP can produce realistic-looking data for a common type of severe convective storm, the supercell. The latter case is significant because it is a record, for over an hour, of volumetric, polarimetric, Doppler-radar data that documents tornadogenesis.

## 4. EXAMPLES

### 4.1 MWR-05XP on 31 May 2007

A low-elevation-angle scan of the supercell shows the classic radar-reflectivity shape (Fig. 3), including a pronounced hook echo. The hook echo is the locus of a broad, cyclonic-vortex signature (Fig. 4). Approaching Doppler velocities along the tip of the hook echo are folded, a bit in excess of  $17.4 \text{ m s}^{-1}$ . While no tornado was observed at this time, a wall cloud and funnel cloud (not shown here), partially embedded in precipitation, were seen.

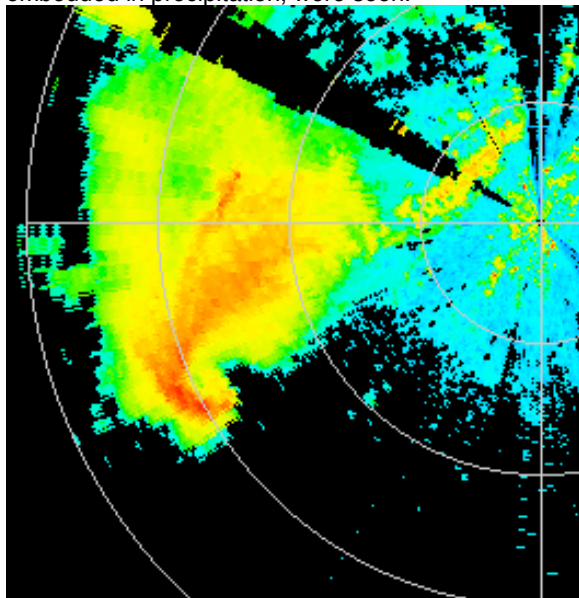


Figure 3. Radar reflectivity of a supercell as seen from MWR-05XP on 31 May 2007 at 1853 CDT from  $\sim 16 \text{ km}$  N of Elkhart, KS. Spacing between range markings is  $16.6 \text{ km}$ . At  $1^\circ$  elevation angle. Color scale not shown.

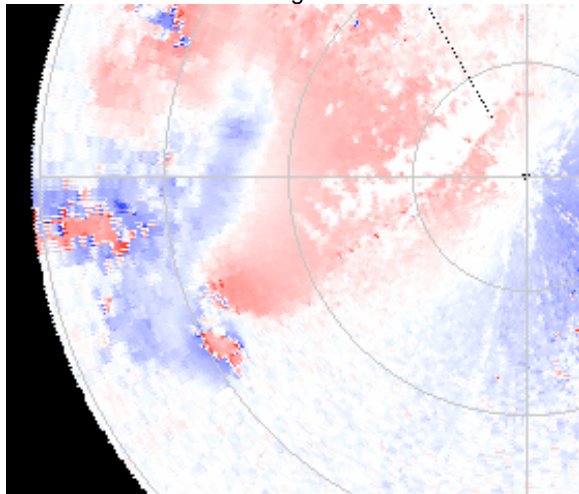


Figure 4. As in Fig. 3, but for Doppler velocities. Color scale not shown. Reds (purples) indicate flow away (toward) the radar. Folding is apparent where deep purple shades change discontinuously to deep red, etc. Folding interval is  $\pm 17.4 \text{ m s}^{-1}$ .

#### 4.2 UMass X-Pol on 4 May 2007

Various images of radar reflectivity and Doppler velocity are shown in subsequent figures, depicting selected aspects of the supercell that produced the Greensburg, KS storm. This storm was scanned from a single location, east of Protection, KS,  $\sim 40 \text{ km}$  SSW of Greensburg, KS. Data collection was nearly continuous from  $\sim 2015 - 2135 \text{ CDT}$ ; Greensburg was hit about 10 - 15 min after data collection had ceased.

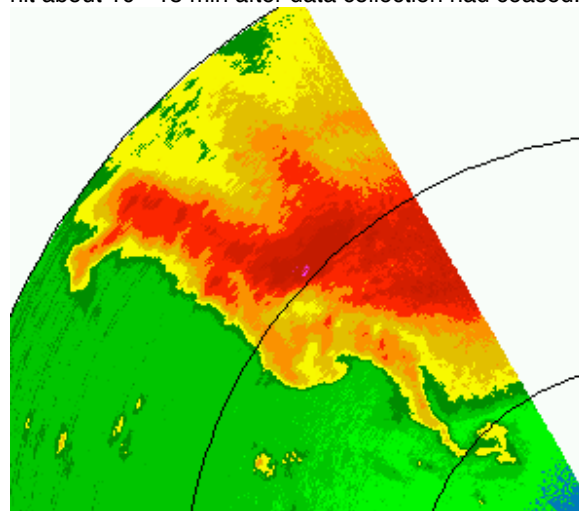


Figure 5. Radar reflectivity of the Greensburg, KS supercell on 4 May 2007, as seen by UMass X-Pol at 2049 CDT at  $4.2^\circ$  elevation angle. Range markings are spaced apart every  $10 \text{ km}$ . The nearest range marker is at  $10 \text{ km}$ . The radar was located  $\sim 4 \text{ km}$  east of Protection, KS.

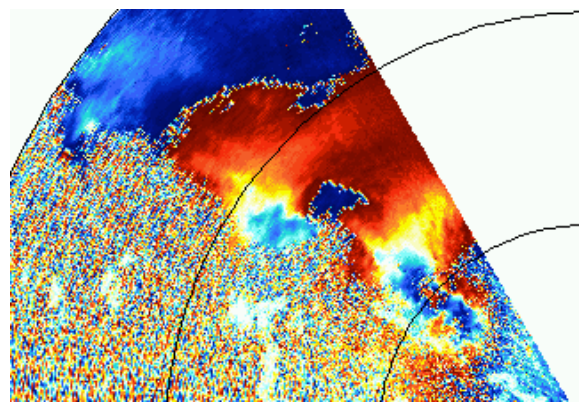


Figure 6. As in Fig. 5, but for Doppler velocity. Reds, yellows (blues, greens) indicate flow away (toward) the radar. Folding interval is  $\pm 19.2 \text{ m s}^{-1}$ ; folding is apparent where deep red shifts discontinuously to purple, etc.

The storm formed to our southwest and tracked northeastward. We chose to remain fixed and sacrifice spatial resolution in favor of temporal continuity by not following the storm. In any event, we had no idea at the time that a large tornado was about to hit a town.

At times the supercell exhibited more than one hook echo. At 2049 CDT as many as three hook echoes were pendant from the SW side of the parent storm (Fig. 5). Two of the hook echoes were associated with

strong cyclonic-vortex Doppler-velocity signatures (Fig. 6).

Later, at 2129 CDT, the supercell took on a classic

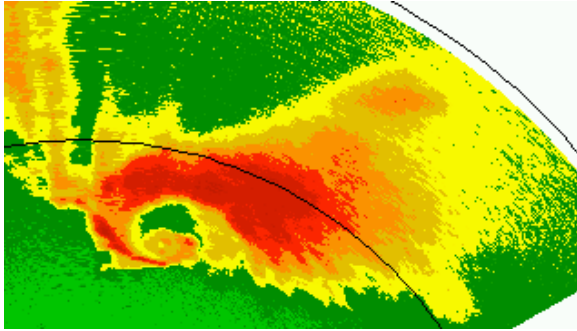


Figure 7. As in Fig. 5, but at 2129 CDT, at 3.2° elevation angle. Inner range ring is at 30 km.

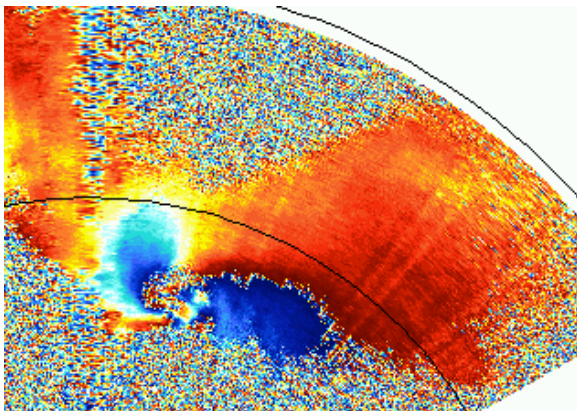


Figure 8. As in Fig. 7, but for Doppler velocity. Scales, etc. as in Fig. 6. Some folding is seen.

appearance (Fig. 7). The hook echo coiled up and an echo-weak hole was evident. The coiled-up hook echo was associated with a strong cyclonic-vortex signature (Fig. 8).

At this same time, at higher elevation angle, the hook echo was composed of short line segments (Fig. 9), i.e., was not curved continuously as at lower elevation angle. Such a feature is sometimes seen in hurricane eyewalls and is thought to indicate disturbances in the flow distributed around the eyewall. In this case, it is surmised that there are disturbances in the mesocyclone. The Doppler-velocity field at the same time displayed some evidence of asymmetries that followed the reflectivity image (Fig. 10). More detailed analyses will be needed to assess these asymmetries further.

The location of the coiled hook and echo-weak hole, and vortex signature were probably coincident with the tornado. Detailed comparisons between the locations of the vortex signatures, et al. with damage tracks will be done later. The vortex signature and weak-echo holes leaned to the NE with height (not shown, but compare Fig. 11 with Fig. 7). At 15.7° elevation angle (~5 km AGL) an echo-weak hole was still evident (Fig. 11). Some scans (not shown) showed a weak area of

reflectivity up to 20° elevation angle, or close to 10 km AGL, at later scans.

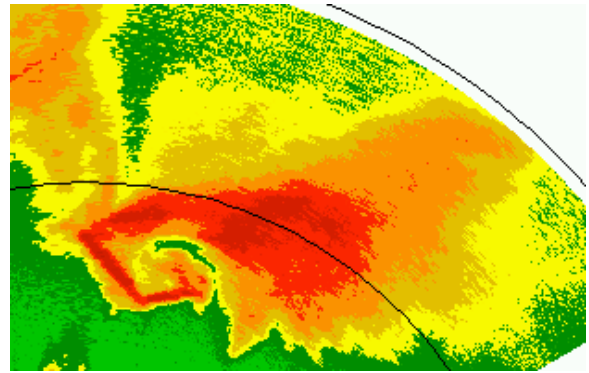


Figure 9. As in Fig. 5, but at 2129 CDT, at 5.7° elevation angle. Inner range ring is at 20 km.

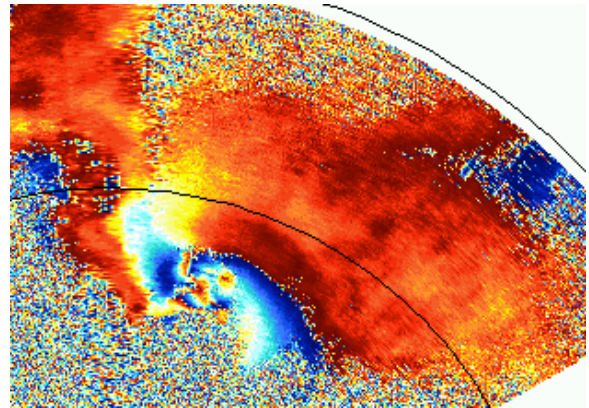


Figure 10. As in Fig. 9, but for Doppler velocity.

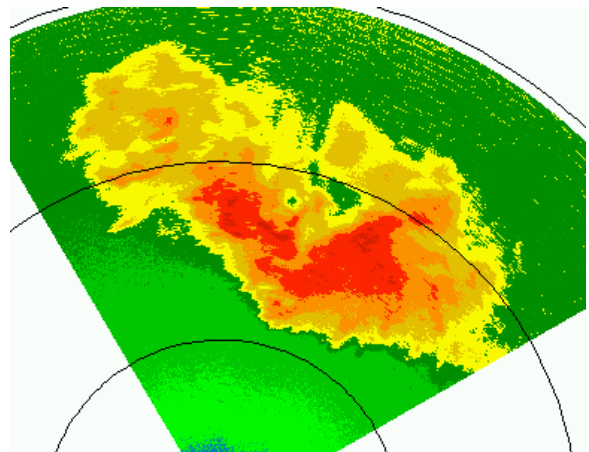


Figure 11. As in Fig. 5, but for 2130 CDT, at 15.7° elevation angle. Inner range ring is at 10 km.

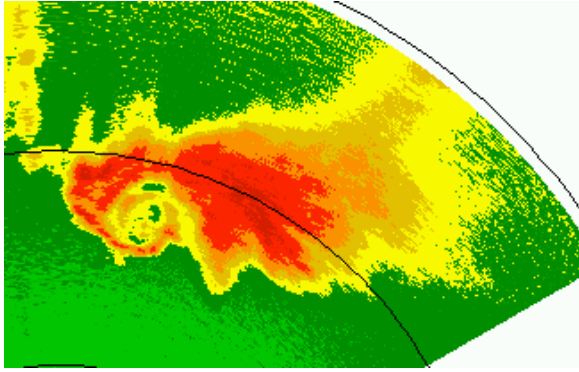


Figure 12. As in Fig. 5, but at 2132 CDT at 3° elevation angle. Inner range marker is at 20 km.

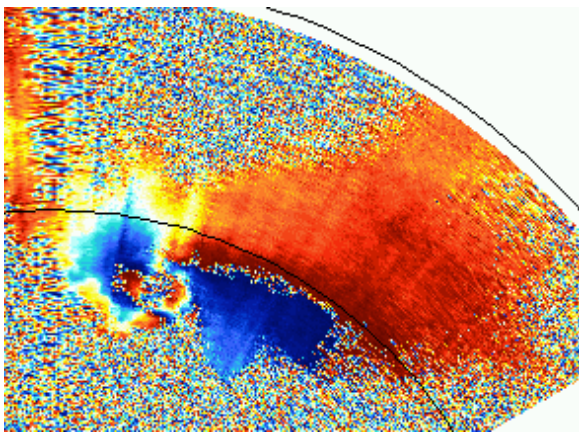


Figure 13. As in Fig. 12, but for Doppler velocity.

At 2132 CDT, evidence was found of multiple vortices. A broad ring of reflectivity, in which there were two holes (Fig. 12) coincided with two cyclonic-vortex signatures (Fig. 13). The final processed data will allow us to look much more closely at the vortex signatures. At about the same time, the tornado, as viewed through intermittent lightning flashes, took on a broad, wedge-like appearance (Fig. 14).



Figure 14. Wide tornado approaching Greensburg, KS at 2134 CDT on 4 May 2007. View to the NE from ~ 20 km NNE of Protection, KS. Photograph © R. Fritchie.

## 5. SUMMARY AND CONCLUSIONS

A wealth of data was collected by the two radars, and will be the focus of much further analysis. Polarimetric data from the UMass X-Pol will be processed and will allow us to distinguish tornado debris rings from precipitation and to distinguish among several types of hydrometeors.

Having a sequence of volume scans every 16 s will allow us to follow storm evolution with unprecedented temporal resolution. Opportunities exist to test out various data assimilation schemes at different temporal resolutions. Next year, with the addition of a stepped motor to the MWR-05XP, we should be able to scan concentrated volumes more rapidly. Improvements to the software will allow us to deploy and take down the MWR-05XP more rapidly.

For some datasets, dual-Doppler analysis will be possible using data from both radars, or from the MWR-05XP and the NSSL PAR, or from the UMass X-Pol and DOW3, a SMART-R, or even a nearby WSR-88D.

## ACKNOWLEDGMENTS

This research was funded by NSF grants ATM-0637148 at OU and ATM-0641201 at UMass. The MWR-05XP radar was provided by CIRPAS at the Naval Postgraduate School and operated under a contract to ProSensing, Inc. from ONR (Office of Naval Research) Other significant participants in this field experiment were the following: Kery Hardwick (UMass), Matt McLinden (UMass), Andy Pazmany (ProSensing), and Paul Buczynski (NPS). Support was also provided by the School of Meteorology at the University of Oklahoma (OU).

## REFERENCES

- Bluestein, H. B., C. C. Weiss, M. M. French, E. Holthaus, R. L. Tanamachi, S. Frasier, and A. L. Pazmany, 2007a: The structure of tornadoes near Attica, Kansas on 12 May 2004: High-resolution, mobile, Doppler-radar observations. *Mon. Wea. Rev.*, **135**, 475 – 506.
- Bluestein, H. B., M. M. French, R. L. Tanamachi, S. Frasier, K. Hardwick, F. Junyent, and A. L. Pazmany, 2007b: Close-range observations of tornadoes in supercells made with a dual-polarization, X-band, mobile Doppler radar. *Mon. Wea. Rev.*, **135**, 1522 – 1543.
- Sandifer, J. B., 2005: Meteorological Measurements with a MWR-05XP Phased Array Radar. *M. S. Thesis*, Naval Postgraduate School, 79 pp.